CONSOLIDATION WITH RADIAL DRAINAGE: OBSERVED AND PREDICTED BEHAVIOUR

CONSOLIDATION PAR ECOULEMENT RADIAL DES EAUX–OBSERVATION ET PREVISION DE COMPORTEMENT

A. Al-Tabbaa

Lecturer, School of Civil Engineering
The University of Birmingham, Birmingham, U.K.

SYNOPSIS

Samples of speswhite kaolin clay were consolidated in the Rowe cell with outward radial drainage in order to investigate the development of excess pore pressure and the variation in void ratio. The experimental program considered both equal and free strain loading conditions and examined the effect of the size of the vertical stress increment. The experimental results showed initial drop and then rise in excess pore pressure above the initial applied value before dissipation and this as a ratio was unaffected by the size of the stress increment. The observed variation in void ratio was negligible for small stress increments and substantial for large increments. The experimental behaviour was satisfactorily modelled using the finite element program CRISP allowing for a smear zone and a finite permeability for the drainage surface. The predictions were more satisfactory for free strain loading and they gave good predictions on successive stress increments.

INTRODUCTION

Horizontal drainage is important in many geotechnical engineering problems involving consolidation. An extensive research programme is at present being carried out at the University of Birmingham into the behaviour of clay during consolidation with horizontal drainage which involves both experimental and theoretical work. Previous numerical analyses using the finite element method [Al-Tabbaa and Muir Wood (1991) and Al-Tabbaa (1992)] predicted phenomena such as initial drop and/or rise in excess pore water pressure in the centre of a consolidating clay mass with radial drainage above the initial applied value before dissipating. Non-uniform distributions in stresses and strains across the sample at the end of consolidation were also predicted. In addition, these analyses suggested that the size of the applied vertical stress increment has a considerable effect on the behaviour of the consolidating clay.

This paper presents the results of experimental work carried out to examine such phenomena and to investigate the effect of factors such as the stiffness of the loading platen and the size of the applied stress increment. These experimental tests were then modelled numerically using the finite element program CRISP [Britto and Gunn (1987)] taking into account the presence of a smear zone and the finite permeability of the drainage boundary. The paper also looks at the difference between experimental and numerical behaviour during three successive stress increments. The observed and predicted behaviour are then compared and aspects of soil behaviour are identified.

EXPERIMENTAL WORK

The experimental problem considered in this paper is the consolidation of a clay sample in a 150mm diameter Rowe cell [Rowe and Barden (1966)] with outward radial drainage. The clay used was speswhite kaolin (LL=69 and PL=38) consolidated in increments from a slurry at a moisture content of 120%. The drainage layer consisted of a 3mm thick porous plastic lining to the cell wall. A typical arrangement of the Rowe cell is shown in Figure 1 and details of setting up and test procedure are given in Head (1985). During each consolidation increment measurements were taken of the excess pore water pressure at the centre of the base of the sample using a pore pressure transducer and of the vertical deformation using a dial gauge.

Tests were carried out under two loading conditions in order to investigate the effect of the stiffness of the loading platen: one using a 5mm thick Aluminium platen to impose the condition of equal vertical strain and the other by applying the loading directly to the top of the sample hence imposing the condition of free vertical strain. In addition, the effect of the size of the applied vertical stress increment on the behaviour of the consolidating clay was investigated by using two different vertical stress increment ratios: a small ratio of 20% and a large ratio of 50% of the initial vertical stress. In total ten tests were carried out and typical results are presented in this paper. The loading was applied incrementally and typical loading profiles are given in Figure 2.

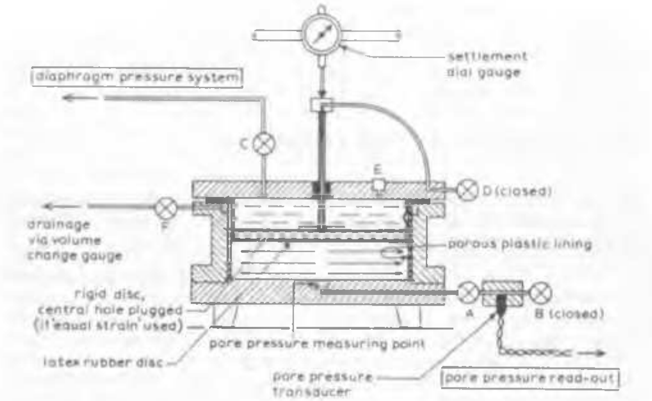

Figure 1. Typical arrangement of the Rowe cell for consolidation test with outward radial drainage [after Head (1985)].

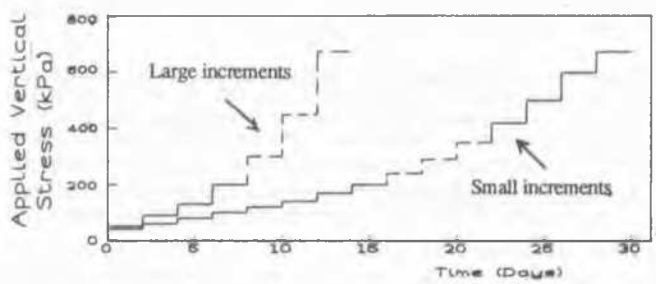

Figure 2. Loading of the tests in terms of applied vertical stress.

The sample was initially subjected to a back pressure of 500kPa and left to reach adequate saturation. The back pressure was then removed and the vertical stress increment applied. Unfortunately, it was not possible at the time the tests were carried out to use a back pressure during the tests and hence at every loading increment the sample was left overnight to reach an adequate level of saturation. At the end of each test the sample was dismantled and concentric rings cut out for moisture content determination.

FINITE ELEMENT ANALYSES

The consolidation problem investigated experimentally was modelled numerically using the finite element program CRISP [Britto and Gunn (1987)]. A mesh representing the problem is shown in Figure 3. Because of symmetry only one half of the problem required modelling and this was done using 144 linear strain quadrilateral elements. Each element had nine integration points at which stresses and strains were calculated. By putting small elements near the drainage and loading boundaries the sharp changes in stresses and strains there were accurately modelled. The vertical stress increment was applied as a uniform pressure to the top face of the top elements.

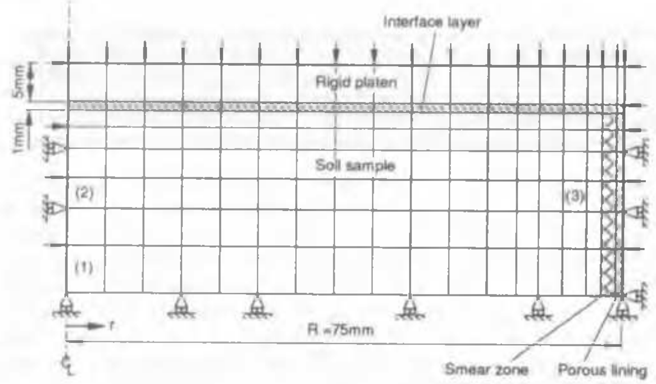

Figure 3. Details of the finite element mesh.

The mesh shown in Figure 3 represents a typical case of an equal vertical strain loading test where the top row of elements represents a rigid platen given the following elastic properties: Young's modulus, $E = 10^5$ kPa and Poison's ratio, $v = 0.3$. It was considered that the value of E chosen to model the rigid platen, which is about 100 times larger that of the soil and 8000 times smaller than that of Aluminium, is appropriate because (i) it is the recommended maximum ratio for stiffness of adjacent elements in CRISP so as to ensure minimum out of balance load errors, (ii) the predicted variation in the vertical deformation across the sample was negligible and (iii) it gave predictions similar to those observed experimentally. In order to obtain uniform deformation along the depth of the sample, a smooth interface was modelled between the soil and the top platen using a 1mm thick row of elements, see Figure 3, with the following elastic properties: E= 1000kPa (similar to that of the soil) and v=0.49 (almost undrained). The vertical and horizontal permeabilities were assigned zero values. When modelling the free strain loading tests the top row of elements was removed and the vertical stress increment was applied directly to the interface layer.

The soil was modelled using the modified Cam clay model [Roscoe and Burland (1968)] which assumes elastic-plastic behaviour on virgin consolidation and a purely elastic response on unloading. The following properties were given to the soil based on experimental work [Al-Tabbaa (1987)]: the slope of the normal compression line in v:ln p' plane λ=0.18; the initial slope of the swelling line in the same plane κ=0.015; the void ratio on the critical state line at p'=1kPa, e_{cs}=2.0; the slope of the critical state line in p':q plane M=0.9 and v=0.3. Vertical and horizontal permeability values of 2×10^{-6}mm/s and 4×10^{-6}mm/s respectively were chosen which correspond to the void ratio at the start of the analyses [Al-Tabbaa and Wood (1987)]. The initial vertical stress chosen was 200kPa. To impose the condition of one-dimensional vertical consolidation in the analyses, a value for the coefficient of lateral earth pressure of K_0=0.78 computed from the modified Cam clay model was used, giving a value for the initial horizontal effective stress of 156kPa. Analyses were carried out for both vertical stress increment ratios of 20% and 50% of the initial vertical stress at every stage. Analyses were also carried out of two subsequent loading increments at the end of the first increment. Hence the increments used were 40, 50 and 60kPa for the small ratio and 100, 150 and 225kPa for the large ratio shown on Figure 2 by the dotted part of the loading steps.

The analyses allowed for a 2mm thick smear zone adjacent to the drainage boundary, see Figure 3, where the permeability of the clay was considered isotropic and equal to the vertical permeability of 2×10^{-6}mm/s. The choice of the thickness of this smear zone is based on observations of some of the samples at the end of a consolidation test under the scanning electron microscope. The drainage layer was modelled using the outer column of elements and given a permeability of 10^{-3}mm/s. For simplicity the drainage layer was assumed to be part of the clay sample in terms of its stiffness. The predictions of the excess pore water pressure presented in this paper are those at the centroid of element marked (1) at the centre of the base of the mesh in Figure 3 which is the nearest element to the position at which the excess pore pressure was measured experimentally.

In the analyses, the flow of pore water and deformation of the soil were fully coupled. In each analysis, the vertical stress increment was applied over a small time period during which the sample remained undrained and after which outward radial drainage was permitted and stresses, strains, excess pore pressures and displacements were calculated over a large number of time increments during consolidation.

RESULTS AND DISCUSSION

Equal Strain Loading

Typical experimental developments of excess pore pressure at the centre of the sample during the three consecutive small and large applied vertical stress increments are shown on Figures 4(a) and (b) respectively, to different scales, together with the corresponding predicted behaviour from the finite element analyses. The general trend in the experimental results was an initial small drop followed by a rise in the excess pore pressure relative to the initial applied value before beginning to dissipate. For the small stress increments shown in Figure 4(a) the range of this observed 'trough' and 'peak' in excess pore pressure was 3-5% and 7-10% of the initial applied value respectively. For the large stress increments in Figure 4(b) these values were slightly smaller with a range of 0-2% and 4-8% for the trough and peak values respectively. For the majority of small stress increments both values seemed to decrease slightly with successive loading while for the large increments the trough increased while the peak decreased on successive loading.

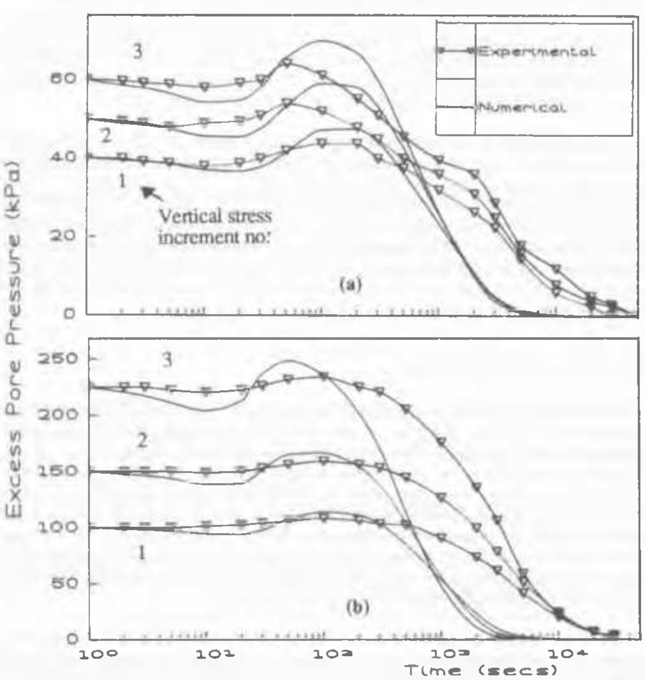

Figure 4. Variation of excess pore water pressure with time for (a) small stress increments and (b) large stress increments.

This general experimental behaviour was predicted in the finite element analyses with the percentages of these initial changes in excess pore pressure, however, being far more pronounced. The predicted range in Figure 4(a) for the trough was 8-10% and for the peak was 16-19% of the initial value for the small stress increments. For the large stress increments in Figure 4(b) these values were 6-10% for the trough and 9-14% for the peak. Hence, the predicted values seem to be about twice those observed experimentally. It is possible that the experimental results were affected by the absence of a back pressure and hence the samples might not have been adequately saturated although other measures were taken to ensure saturation and this is now the subject of a current research project. The analyses agree with the experimental results in showing that the initial changes in excess pore pressure as a percentage of the initial applied value decreased slightly under large stress increments. Good agreement was also found between the experimental and numerical results regarding the time at which the trough and peak values of the excess pore pressure were reached with the experimental time being slightly earlier in a number of cases.

Subsequently, slower dissipation of excess pore pressure was observed compared to that predicted. This was probably due to the fact that the permeability of the clay is continuously decreasing as the sample consolidates while the finite element analyses can only allow for a constant permeability throughout a consolidation analysis. Better agreement should be obtained if variable permeability is incorporated into CRISP.

Figures 5(a) and (b) show typical variation of void ratio across the sample at the end of a consolidation test for small and large stress increments respectively where the radius, r, is plotted as a ratio (r/R) of the internal radius of the Rowe cell, R (see Figure 3). The experimental results on Figure 5(a) show the highest void ratio to be at the centre and the lowest at the edge of the sample with a maximum difference of 0.04. The finite element analyses on the same Figure show a reasonably uniform sample at the end of the first increment and a small variation at the end of the third increment of 0.009 across the sample. Assuming that this variation is cumulative, at the end of a complete test of fifteen small stress increments, see Figure 2, the analysis is likely to yield similar variation to that observed experimentally.

The experimental results on Figure 5(b) show that the effect of large stress increments is to produce large variation in void ratio with a typical maximum variation of 0.11 between the centre and edge of the sample. The finite element analyses support this experimental finding and show how the non-uniformity in void ratio develops dramatically on successive applications of large stress increments. At the end of the third increment, the predicted maximum variation was 0.076, and hence with a complete test of seven large increments, the predicted variation is likely to be greater than the observed.

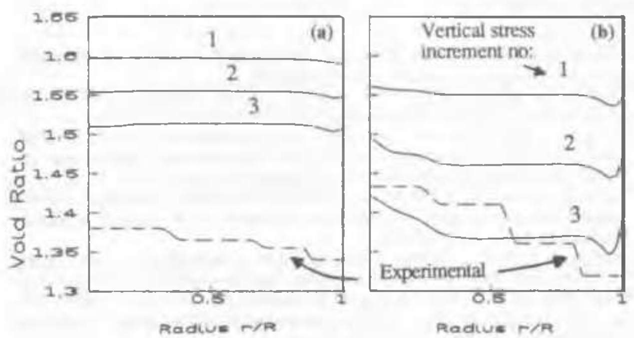

Figure 5. Distribution of void ratio across the sample for (a) small stress increments and (b) large stress increments.

Free Strain Loading

Figures 6(a) and (b) show the development of excess pore pressure with time at the centre of the sample under free strain loading during three small and large successive stress increments respectively. The general pattern of an initial drop and subsequent rise in excess pore pressure observed in the equal strain loading tests was also observed here. For the small stress increments, Figure 5(a) shows that the experimental and finite element range for the trough values was 8-11% and 12-14% and for the peak was 3-9% and 4-9% respectively. For the large stress increments, Figure 6(b) shows slightly smaller ranges of 8-9% and 10-11% for the trough and 2-5% and 3-6% for the peak respectively. These results suggest much closer agreement between the experimental and finite element analyses. The time at which these optimum values were reached did not seem to vary experimentally but seems to reduce slightly in the finite element analyses with subsequent increments.

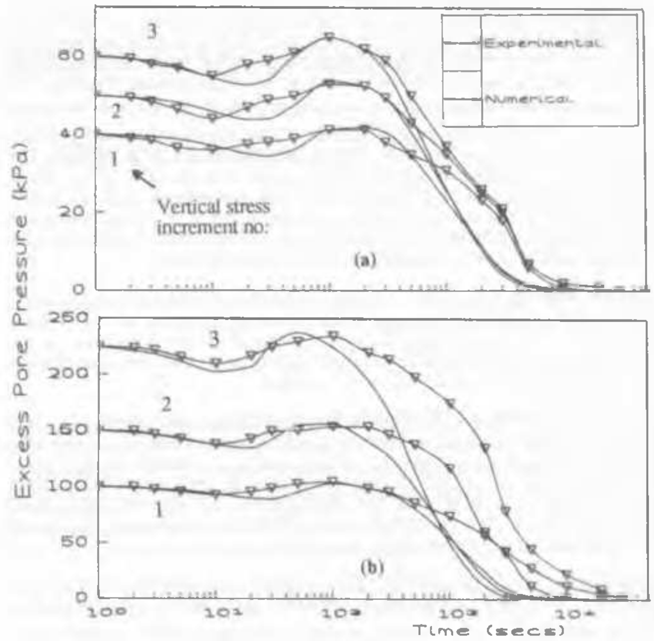

Figure 6. Variation of excess pore pressure with time for (a) small stress increments and (b) large stress increments.

The variation in void ratio is shown on Figures 7(a) and (b) for small and large stress increments respectively. The experimental variation in Figure 7(a) shows a reasonably uniform sample at the end of a complete test of small stress increments with a maximum variation of 0.01. The finite element analyses predicted a reasonably uniform sample at the end of three consecutive stress increments. On the other hand, Figure 7(b) for large stress increments shows a maximum experimental difference of 0.1 between the centre and edge of the sample at the end of a typical test. At the end of the third increment in the finite element analyses the variation was 0.04. Assuming that this response is cumulative, at the end of a complete test of seven large increments the variation is likely to be double that obtained after three increments and hence is similar to that observed experimentally.

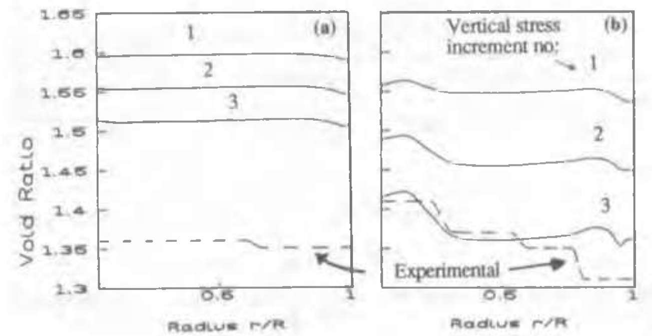

Figure 7. Distribution of void ratio across the sample for (a) small stress increments and (b) large stress increments.

General Discussion

The experimental excess pore pressure results presented in this paper are typical of about 70% of the test increments. For the remaining 30%, the experimental results showed no initial drop or rise in the excess pore pressure i.e. remaining equal to the initial applied value before starting to dissipate in a similar fashion to the results presented here. It is not possible at this stage to explain this discrepancy.

The numerical modelling of the consolidation behaviour was less satisfactory for the equal strain loading than for the free strain loading tests. One of the reasons for this could be the way in which the condition of equal vertical strain was imposed in the finite element analyses for the equal strain condition. Finite element analyses were carried out to look at the effect of using a stiffness for the loading platen similar to that of Aluminium of $8x10^7$kN/m^2, instead of that actually used in the analyses of 10^5kN/m^2. These analyses predicted no initial trough in excess pore pressure, which perhaps agrees with some of the experimental results, and subsequently a peak of up to 60% of the initial applied value which was much higher than what was achieved experimentally. The author is at present investigating alternative methods of imposing equal strain loading conditions in the finite element analyses which would allow the use of a realistic i.e. very high stiffness for the loading platen.

The results presented here showed that initial changes in excess pore pressure were slightly smaller during large stress increments compared to small stress increments. However, these changes, compared to the difference in the increment size, were negligible and in general it can be said that these changes are unaffected by the size of the stress increment.

The experimental results presented in this paper indicate that free strain loading produces 'slightly' less non-uniformity in void ratio at the end of consolidation than equal strain loading. The finite element analyses predicted a similar degree of non-uniformity for both loading conditions. In both cases, small stress increments produced negligible non-uniformity in void ratio while large stress increments produced large non-uniformity. Therefore, small stress increments should be used if a uniform sample is required.

Non-uniformity in void ratio implies non-uniformity in effective stresses. It is, therefore, of interest to look at the predicted stress paths in terms of the mean effective stress, $p'=(\sigma_z'+\sigma_r'+\sigma_\theta')/3$, and the deviator stress, $q=[\{(\sigma_z'-\sigma_r')^2+(\sigma_r'-\sigma_\theta')^2+(\sigma_\theta'-\sigma_z')^2\}/2]^{1/2}$ where σ_z', σ_r' and σ_θ' are the effective vertical, radial and circumferential stresses respectively. These stress paths are plotted on Figures 8(a) and (b) for small and large stress increments respectively, where the scale in (a) is about three times that in (b) and the beginning and end of each increment are identified. These figures show the stress paths followed by two elements: one at the centre, marked (2), and the other near the edge of the sample marked (3), see Figure 3. These stress paths clearly show how different the behaviour is between the two points and how at the end of each consolidation step, the values of p' and q are different. This difference seems to increase on successive stress increments. These figures also show that for small increments, both equal and free strain loading produced similar results while, during large stress increments, equal strain loading showed a bigger difference in p' and q between the two points.

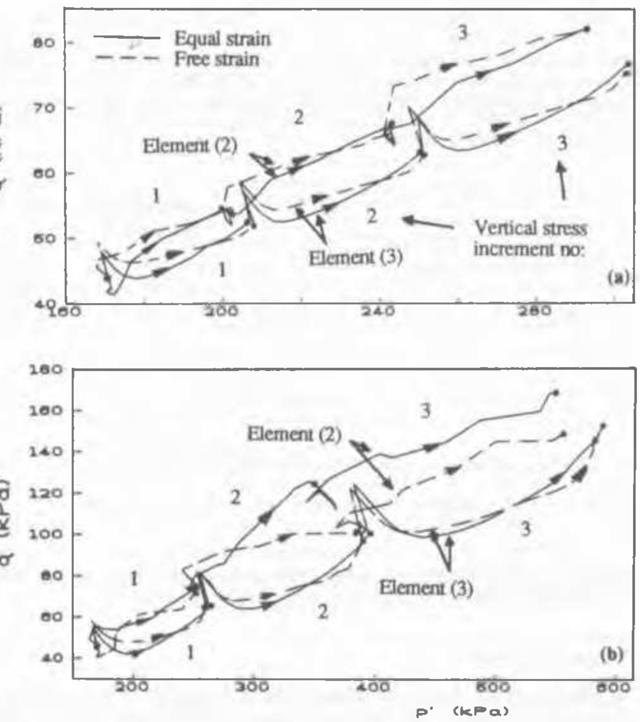

Figure 8: Effective stress paths in p':q space for (a) small and (b) large stress increments.

Based on the results presented here, it can be said that the consolidation behaviour on successive stress increments was reasonably predicted by the finite element analyses. The modified Cam-clay model is, therefore, considered satisfactory for modelling virgin compression of clay under radial drainage conditions. Part of the present programme is to investigate the behaviour of the clay during unloading. It was demonstrated [Al-Tabbaa and Wood (1989)] that the behaviour of clay on unloading is elastic-plastic and hence a similar response in terms of excess pore pressure and void ratio seen on loading might, in general terms, be expected on unloading. In this case, the modified Cam-clay model will be inappropriate to model the behaviour during unloading as it assumes a purely elastic response. The experimental results of tests during unloading will be valuable in order to shed light on this aspect of soil behaviour. The author is at present involved in implementing the model developed by Al-Tabbaa and Wood (1989) into CRISP so that soil behaviour on unloading can be adequately modelled.

CONCLUSIONS

The experimental results presented in this paper confirm results of previous finite element analyses of an initial trough and peak in excess pore pressure before dissipation. This behaviour was more pronounced under equal strain than free strain loading. The change in excess pore pressure as a percentage of the initial applied value was found to be unaffected by the size of the applied vertical stress increment. Some variation in void ratio across the sample occurred at the end of all tests which was negligible when small stress increments were applied but considerable with large increments.

The experimental consolidation behaviour during three successive stress increments presented here was satisfactorily modelled using the finite element program CRISP allowing for a smear zone and a finite permeability for the drainage boundary. The analyses were, however, more satisfactory for free strain loading and showed that the modelling of the rigid loading platen requires further investigation. Based on the investigation carried out in this paper it can be said that consolidation with radial drainage causes non-uniformities in stresses and strains which may need to be taken into account when designing structures on consolidating clay. It was demonstrated that the degree of this non-uniformity depends on the loading conditions and the size of the stress increment.

REFERENCES

Al-Tabbaa, A. (1987). Permeability and stress-strain response of speswhite kaolin. PhD Thesis, University of Cambridge.

Al-Tabbaa, A. and Wood, D. M. (1987). Some measurements of the permeability of kaolin. *Geotechnique* 37(4): 499-503.

Al-Tabbaa, A. and Wood, D.M. (1989). An experimentally based 'bubble' model for clay. *Proceedings of the IIIrd International Symposium on Numerical Models in Geomechanics*, Niagara Falls, pp 91-99.

Al-Tabbaa, A. and Muir Wood, D. (1991). Horizontal drainage during consolidation: insights gained from analyses of a simple problem. *Geotechnique* 41(4): 571-585.

Al-Tabbaa, A. (1992). Finite element analyses of consolidation with radial peripheral drainage. *Proceedings of the IVth International Symposium on Numerical Models in Geomechanics*, Swansea, pp 441-451.

Britto, A. M. and Gunn, M. J. (1987). *Critical state soil mechanics via finite elements*. Ellis Horwood Ltd, Chechester.

Head, K. H. (1985). *Manual for soil laboratory testing*. Vol. 3, Chapter 24, Pentech Press, London.

Roscoe, K. H. and Burland, J. B. (1968). On the generalised stress-strain behaviour of 'wet' clay. *Engineering Plasticity (edited by J Heyman and P A Leckie)*, Cambridge University Press, pp 535-609.

Rowe, P. W. and Barden, L. (1966). A new consolidation cell. *Geotechnique* 16(2):162-170.